

# **JAXA Research and Development Report**

---

## **Direct simulation Monte Carlo study of rotational relaxation of nitrogen using classical trajectory calculations and modified statistical inelastic cross-section model**

**Katsuhisa KOURA, Kinuyo NAKAMURA and Yasuhiro MIZOBUCHI**

**July 2007**

**Japan Aerospace Exploration Agency**



# JAXA Research and Development Report

## Direct simulation Monte Carlo study of rotational relaxation of nitrogen using classical trajectory calculations and modified statistical inelastic cross-section model

Katsuhisa KOURA<sup>\*1</sup>, Kinuyo NAKAMURA<sup>\*1</sup> and Yasuhiro MIZOBUCHI<sup>\*1</sup>

<sup>\*1</sup> Computational Science Research Group, Institute of Aerospace Technology,  
Japan Aerospace Exploration Agency

July 2007

Japan Aerospace Exploration Agency



# Direct simulation Monte Carlo study of rotational relaxation of nitrogen using classical trajectory calculations and modified statistical inelastic cross-section model\*

Katsuhisa KOURA\*<sup>1</sup>, Kinuyo NAKAMURA\*<sup>1</sup> and Yasuhiro MIZOBUCHI\*<sup>1</sup>

## ABSTRACT

Direct simulation Monte Carlo (DSMC) calculations of the rotational relaxation of nitrogen in an isothermal bath and through a normal shock wave are performed using classical trajectory calculations (CTC) and an improved intermolecular potential in order to make a physically accurate database for the assessment and improvement of DSMC rotational relaxation models. The statistical inelastic cross-section (SICS) model is modified by taking the total scattering cross section as the variable soft sphere (VSS) cross section and calibrated so that the rotational temperature relaxation in an isothermal bath compares reasonably with the CTC–DSMC data over an appropriate range of bath temperatures. The modified SICS (MSICS) model is applied to the DSMC calculation of the rotational relaxation of nitrogen through a normal shock wave. Comparisons of the MSICS results with the CTC–DSMC data and experimental measurements indicate that the MSICS model improves the physical accuracy of the SICS model.

**Keywords :** Rotational relaxation model, Direct simulation Monte Carlo method, Classical trajectory calculations, Normal shock wave

## I. INTRODUCTION

Direct simulation Monte Carlo (DSMC) calculations<sup>1</sup> of the rotational relaxation in rarefied gas flows are mostly performed using some computationally efficient phenomenological models of Borgnakke–Larsen type,<sup>2</sup> while further studies<sup>3–5</sup> were made to improve the physical accuracy of DSMC rotational relaxation models. Wysong and Wadsworth<sup>6</sup> assessed the phenomenological models by comparing DSMC calculations of the rotational relaxation of nitrogen in isothermal and adiabatic baths and through normal shock waves with the bath calculations using the state-to-state rate constants of the quasiclassical fitting law (qECSE model)<sup>7</sup> and with the experimental shock wave measurements.<sup>8</sup> It is indicated that the physical accuracy of the phenomenological models is not satisfactory.

In previous papers,<sup>9–11</sup> the classical trajectory calculations (CTC) for the collision of two rigid diatomic molecules have been coupled with the DSMC method. The CTC–DSMC method provides a physically accurate database for the assessment and improvement of DSMC rotational relaxation models if an accurate intermolecular potential is used. For nitrogen, an improved potential energy surface (PES) was constructed by van der Avoird et al. (AWJ)<sup>12</sup> and some of the AWJ potential parameters were readjusted by Cappelletti et al.<sup>13</sup> to yield the PES8 potential, which has been verified to be sufficiently accurate by comparing with various experimental measurements.

In the present paper, the PES8 potential is used for CTC–DSMC calculations of the rotational relaxation of nitrogen in an isothermal bath and through a normal shock wave. The bath calculation is made over a wide range of bath temperatures 100–10000K (regardless of

---

\* 平成 19 年 6 月 12 日受付 (received 12 June, 2007)

\*<sup>1</sup> Computational Science Research Group, Institute of Aerospace Technology, Japan Aerospace Exploration Agency

the vibrational excitation) to obtain an appropriate set of rotational relaxation data. Because the PES8 potential requires a large amount of computation time, the shock wave calculation is made only for a high Mach number of 12.9 to see the agreement with the experimental measurements of Robben and Talbot.<sup>8</sup>

The statistical inelastic cross-section (SICS) model was previously proposed<sup>3,14,15</sup> as a phenomenological cross-section model, where the elastic cross section is taken to be the variable soft sphere (VSS) cross section.<sup>16,17</sup> Considering that the VSS model is valid for molecules with rotational degrees of freedom, in the present paper, the SICS model is modified by taking the total scattering cross section as the VSS cross section and calibrated so that the rotational temperature relaxation in an isothermal bath compares reasonably with the CTC-DSMC data over an appropriate range of bath temperatures. The modified SICS (MSICS) model is applied to the DSMC calculation of the rotational relaxation of nitrogen through a normal shock wave to compare the MSICS results with the CTC-DSMC data and experimental measurements.<sup>8</sup> The details of the null-collision DSMC procedure<sup>18,19</sup> for the MSICS model are described for the convenience of a simulation replication.

## II. CTC-DSMC CALCULATIONS

### A. Improvement on CTC-DSMC method

The present CTC-DSMC calculations are performed using the CTC-DSMC method described in Ref. 9, where the classical trajectory calculations for the collision of two rigid diatomic molecules are made by solving a set of canonical equations of motion with a rigid rotor constraint in the Cartesian coordinate system using a variable-step eighth-order Runge-Kutta formula. In order to improve the physical accuracy of CTC-DSMC data for nitrogen, the intermolecular potential is taken as the PES8 potential. The maximum impact parameter  $b_{\max}$  for the PES8 potential may be taken as that derived<sup>9,20</sup> from the attractive term of the isotropic Lennard-Jones potential using the truncation of the scattering deflection angle less than  $0.05^\circ$ ,

$$b_{\max} = \max[3\sigma_{\text{LJ}}(24\varepsilon_{\text{LJ}}/\varepsilon)^{1/6}, 3\sigma_{\text{LJ}}], \quad (1)$$

with the collision diameter  $\sigma_{\text{LJ}}=3.681\text{\AA}$  and the well depth  $\varepsilon_{\text{LJ}}/k=91.5\text{K}$  for nitrogen, where  $\varepsilon$  is the relative translational energy and  $k$  is Boltzmann's constant. For  $b_{\max}$  given

by Eq. (1), the initial intermolecular separation  $R_0(>b_{\max})$  may be taken as

$$R_0 = 1.1b_{\max}. \quad (2)$$

It is noted that Eqs. (1) and (2) are more accurate than Eqs. (18) and (20) of Ref. 9 and should be substituted for them.

Because experimental and theoretical rotational distribution functions are often presented for the discrete rotational energy, the continuous rotational energy  $E_r$  is quantized by a commonly used method<sup>21</sup> to obtain the rotational distribution function  $y_j$  of even quantum numbers  $j$  for nitrogen. If  $E_r$  lies between the discrete rotational energies  $E_{j-1}$  and  $E_{j+1}$ , then  $E_r$  is ascribed to  $E_j=k\theta_r j(j+1)$ , where  $\theta_r$  is the characteristic rotational temperature taken to be 2.875K for nitrogen; i.e., the quantum number  $j$  is obtained from the continuous quantum number  $j_c$  defined by  $E_r=k\theta_r j_c(j_c+1)$  as

$$\begin{aligned} j_c &= [-1 + (1 + 4E_r/k\theta_r)^{1/2}]/2, \\ j &= 2 \times \text{int}[(j_c + 1)/2], \end{aligned} \quad (3)$$

where  $\text{int}[X]$  denotes the integer part of  $X$ .

### B. Rotational relaxation of nitrogen in isothermal bath

The CTC-DSMC calculation of the rotational relaxation of nitrogen in an isothermal bath, where the molecular number  $N$  is taken to be 10000, is performed for the zero initial rotational energy (temperature) at the bath translational temperature  $T=100, 300, 1000, 3000$ , and  $10000\text{K}$ . The velocity distribution function is fixed to be the Maxwellian at the bath temperature and, therefore, the molecular velocities before collision are chosen from the Maxwell distribution function and those after collision are discarded. The rotational temperature is obtained to be  $T_r=\langle E_r \rangle/k$  from the mean rotational energy  $\langle E_r \rangle$  of all the molecules in the bath.

The relaxation of the rotational temperature  $T_r$  normalized by  $T$  is shown in Fig. 1, where the time  $t$  is normalized by the collision time  $t_0=[n\pi\sigma_{\text{LJ}}^2(2kT/m)^{1/2}]^{-1}$ ,  $n$  and  $m$  being the molecular number density and mass, respectively. It is indicated that the rotational relaxation becomes slower at the higher bath temperature in accordance with the well-known fact that the rotational collision number increases with the increase in the translational temperature.

The relaxation of the rotational distribution function  $y_j$  normalized by the degeneracy  $g_j=2j+1$  relative to that of

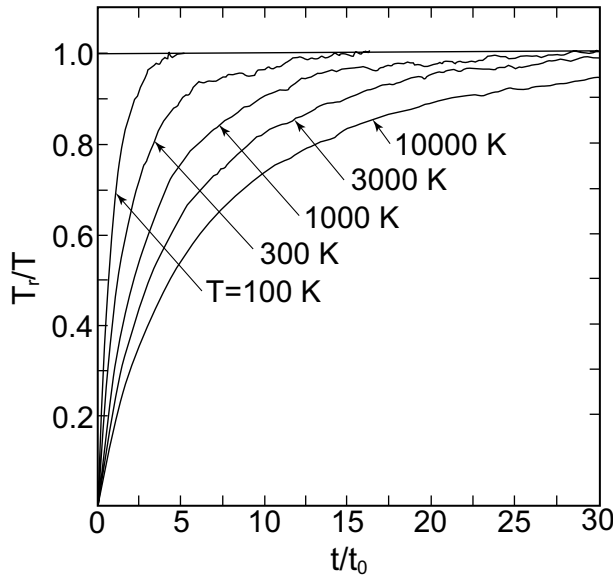


FIG. 1. Rotational temperature relaxation in an isothermal bath obtained by CTC-DSMC calculation with the PES8 potential for the zero initial rotational temperature at the bath temperature  $T=100, 300, 1000, 3000$ , and  $10000\text{K}$ .

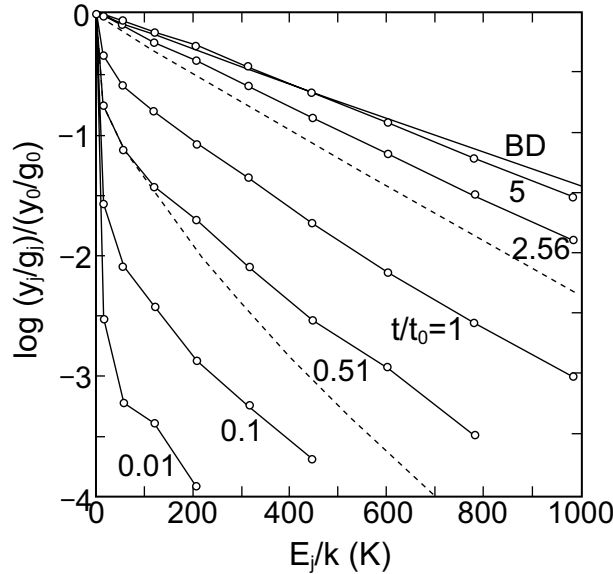


FIG. 2. Relaxation of rotational distribution function in an isothermal bath obtained by CTC-DSMC calculation with the PES8 potential ( $\circ$ ) for the zero initial rotational temperature at the bath temperature  $T=300\text{K}$ . The rotational distribution function obtained by solving the master rate equation with the qECSE rate constants (---, Ref. 6) for the initial rotational temperature of  $2.9\text{K}$  at  $T=300\text{K}$  is plotted at the time  $t=\tau_e$  ( $t/t_0=0.51$ ) and  $t=5\tau_e$  ( $t/t_0=2.56$ ). BD denotes the Boltzmann distribution function at the bath temperature.

the ground level,  $(y_i/g_i)/(y_0/g_0)$ , is presented in Fig. 2 for the bath temperature  $T=300\text{K}$ . It is indicated that the rotational distribution function relaxes to the Boltzmann distribution function (straight line) via a bimodal form represented approximately by the merging of two Boltzmann distribution functions. Wysong and Wadsworth<sup>6</sup> obtained the rotational distribution function by solving the isothermal master rate equation with the qECSE rate constants for the initial rotational temperature of  $2.9\text{K}$  at  $T=300\text{K}$ . The qECSE rotational distribution function is plotted at the time  $t=\tau_e$  ( $t/t_0=0.51$ ) and  $t=5\tau_e$  ( $t/t_0=2.56$ ), where  $\tau_e$  is the collision time evaluated to be  $2.2 \times 10^{-10}\text{s}$  for  $n=2.687 \times 10^{19}\text{cm}^{-3}$ . It is observed that the rotational relaxation is somewhat slower for the qECSE model than for the PES8 potential. The discrepancy between the qECSE model and the PES8 potential was also indicated by Wysong<sup>22,23</sup> and may be ascribed to some uncertainties of the qECSE model<sup>7</sup> without rotation-to-rotation transitions.

### C. Rotational relaxation of nitrogen through normal shock wave

The CTC-DSMC calculation of the rotational relaxation of nitrogen through a normal shock wave is made for the upstream Mach number  $M_1=12.9$  and temperature  $T_1=9.15\text{K}$  to see the agreement with the experimental measurements of Robben and Talbot.<sup>8</sup> The cell width  $\Delta x$  along the streamwise coordinate  $x$  normalized by the upstream free path  $\lambda_1=(n_1\pi\sigma_{LJ}^2)^{-1}$ ,  $n_1$  being the upstream number density, is taken to be  $\Delta x/\lambda_1=0.1$  and the average molecular number per cell is taken to be about 100.

The profiles of normalized number density  $\bar{n}=(n-n_1)/(n_2-n_1)$ , translational temperature  $\bar{T}=(T-T_1)/(T_2-T_1)$ , and rotational temperature  $\bar{T}_r=(T_r-T_1)/(T_2-T_1)$  are shown in Fig. 3 as compared with the measured data of  $\bar{n}$  and  $\bar{T}_r$ , where the subscripts 1 and 2 refer to the upstream and downstream conditions of the shock wave, respectively, and the position  $x$  is normalized by the sonic free path  $L^*=\eta(T^*)/\rho u$  employed in Ref. 8 with the viscosity coefficient  $\eta(T^*)$  at the adiabatic sonic temperature  $T^*$  and the constant mass flux  $\rho u$ . The CTC-DSMC profiles obtained previously using the extended Morse (EM) potential<sup>9</sup> are also plotted. A comparison of the profiles between the PES8 and EM potentials indicates that the rotational relaxation is a little faster and the agreement with the measured profiles is even better for the PES8 potential than

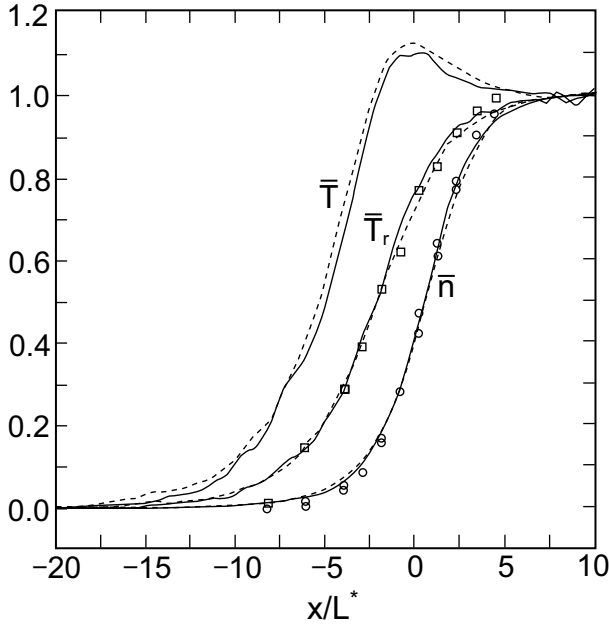


FIG. 3. Profiles of normalized number density ( $\bar{n}$ ) and translational ( $\bar{T}$ ) and rotational ( $\bar{T}_r$ ) temperatures through a Mach 12.9 shock wave obtained by CTC-DSMC calculation with the PES8 potential (—) as compared with the experimental data (Ref. 8) of  $\bar{n}$  (○) and  $\bar{T}_r$  (□) and the CTC-DSMC profiles for the extended Morse potential (---, Ref. 9).

for the EM potential. It is noted that in the upstream portion of the shock wave the CTC-DSMC rotational temperature begins to rise gradually before the steep rise of the measured data. The discrepancy in the upstream portion may possibly be caused by low temperature uncertainties of the CTC-DSMC calculation without quantum effects or of the experimental measurements.

The relaxation of the relative rotational distribution function ( $y_i/g_i$ )/( $y_0/g_0$ ) is shown in Fig. 4 as compared with the experimental measurements. The rotational distribution function relaxes to the Boltzmann distribution function via a bimodal form represented approximately by the merging of two Boltzmann distribution functions at the upstream and downstream temperatures in good agreement with the experimental data except in the upstream portion of the shock wave,  $x/L^* = -10.3$  (3.0 turns) and  $-8.2$  (3.5 turns). The discrepancy in the upstream portion may also be attributable to low temperature uncertainties of the experimental measurements with the straight line extrapolation at the high quantum numbers ( $j > 6$ ) [see Fig. 5(a) of Ref. 8] or of the CTC-DSMC calculation.

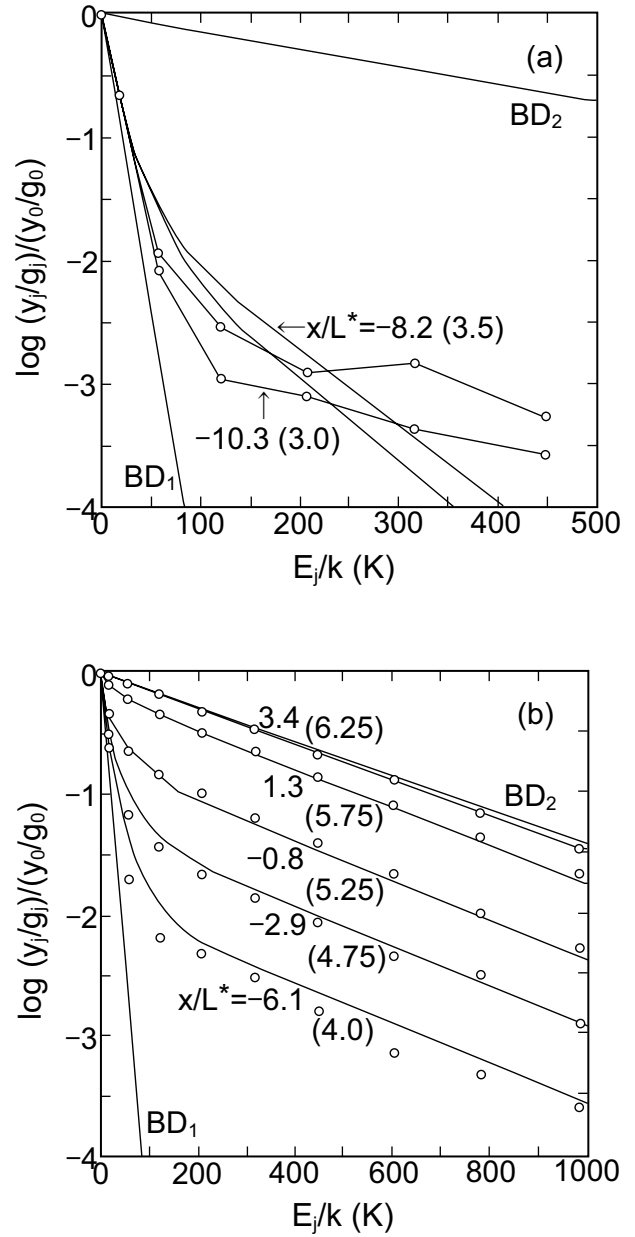


FIG. 4. Relaxation of rotational distribution function through a Mach 12.9 shock wave obtained by CTC-DSMC calculation with the PES8 potential (○) as compared with the experimental data (—, Ref. 8). The value in parentheses is the measured position in the unit of turns.  $BD_1$  and  $BD_2$  denote the Boltzmann distribution functions at the upstream and downstream temperatures, respectively.



### III. MSICS CALCULATIONS

#### A. MSICS model

The SICS model for the continuous rotational energy<sup>14</sup> is modified by taking the total scattering cross section  $\sigma_t(\epsilon)$  as the VSS cross section<sup>16,17</sup>; i.e.,

$$\sigma_t(\epsilon) = c\epsilon^{-\omega}. \quad (4)$$

The probability density function  $P(\chi)$  of the scattering deflection angle  $\chi$  is also given by the VSS model<sup>3,16</sup>

$$P(\chi) = \alpha \cos^{2\alpha-1}(\chi/2) \sin(\chi/2). \quad (5)$$

The values of the VSS parameters  $c$ ,  $\omega(\leq 0.5)$ , and  $\alpha$  for nitrogen are given in Table II of Ref. 17; i.e.,  $c = 499.5$ ,  $\omega = 0.359$ , and  $\alpha = 1.784$  for low temperatures  $T \leq 300\text{K}$  and  $c = 134.4$ ,  $\omega = 0.172$ , and  $\alpha = 1.362$  for high temperatures  $T > 300\text{K}$ .

The rotationally inelastic cross section  $\Delta\sigma_r(\epsilon; \xi_1, \xi_1'; \xi_2, \xi_2')$  for the rotational energy changes from  $\xi_1$  to  $\xi_1'$  in the range of  $\Delta\xi_1'$  and from  $\xi_2$  to  $\xi_2'$  in the range of  $\Delta\xi_2'$  between the collision molecules 1 and 2 with the rotational energies  $\xi_1$  and  $\xi_2$  before collision, respectively, is expressed in the statistical form

$$\Delta\sigma_r(\epsilon; \xi_1, \xi_1'; \xi_2, \xi_2') / \sigma_t(\epsilon) = \zeta_r(E, \xi_1', \xi_2') \Delta\xi_1' \Delta\xi_2', \quad (6)$$

where  $E$  is the total energy given by

$$\begin{aligned} E &= \epsilon + \xi_1 + \xi_2 \\ &= \epsilon' + \xi_1' + \xi_2', \end{aligned} \quad (7)$$

$\epsilon$  and  $\epsilon'$  being the relative translational energies before and after collision, respectively, and  $\zeta_r(E, \xi_1', \xi_2')$  is the rotational cross-section function satisfying the obvious condition

$$\zeta_r(E, \xi_1', \xi_2') = 0, \xi_1' + \xi_2' \geq E. \quad (8)$$

The functional form of  $\zeta_r(E, \xi_1', \xi_2')$  is determined from the principle of detailed balancing<sup>14</sup>

$$\epsilon \sigma_t(\epsilon) \zeta_r(E, \xi_1', \xi_2') = \epsilon' \sigma_t(\epsilon') \zeta_r(E, \xi_1, \xi_2) \quad (9)$$

to be

$$\zeta_r(E, \xi_1', \xi_2') = C(E)(E - \xi_1' - \xi_2') \sigma_t(E - \xi_1' - \xi_2'). \quad (10)$$

Using Parker's rotational energy gain function<sup>3,24,25</sup>  $\Delta E_r(\epsilon)$ , the function  $C(E)$  is determined from the rotational energy gain relation<sup>14</sup>

$$2\Delta E_r(\epsilon) \sigma_t(\epsilon) = \int [\Delta\sigma_r(\epsilon; 0, \xi_1'; 0, \xi_2') / \Delta\xi_1' \Delta\xi_2'] (\xi_1' + \xi_2') d\xi_1' d\xi_2' \quad (11)$$

to be

$$C(E) = (2 - \omega)(3 - \omega)(4 - \omega) \Delta E_r(E) / [E^4 \sigma_t(E)]. \quad (12)$$

$\Delta E_r(E)$  for the VSS model is given by<sup>25</sup>

$$\Delta E_r(E) = \{E/(1 + \alpha) + (\pi^{3/2}/2)[\Gamma(1 + \alpha)/\Gamma(3/2 + \alpha)](E E^*)^{1/2} + (2 + \pi^2/4)E^*\}/Z_r^\infty, \quad (13)$$

where  $E^*$  is the potential well depth taken to be  $\epsilon_{LJ}$  and  $Z_r^\infty$  is an adjustable parameter corresponding to Parker's limiting rotational collision number.<sup>24</sup>

Because the total rotational cross section defined by

$$\sigma_r(\epsilon, \xi_1, \xi_2) = \int [\Delta\sigma_r(\epsilon; \xi_1, \xi_1'; \xi_2, \xi_2') / \Delta\xi_1' \Delta\xi_2'] d\xi_1' d\xi_2' \quad (14)$$

is given by

$$\sigma_r(\epsilon, \xi_1, \xi_2) = [(4 - \omega) \Delta E_r(E) / E] \sigma_t(\epsilon), \quad (15)$$

a modification is required to satisfy the obvious condition

$$\sigma_r(\epsilon, \xi_1, \xi_2) \leq \sigma_t(\epsilon). \quad (16)$$

It may be a consistent modification to represent  $\sigma_r(\epsilon, \xi_1, \xi_2)$  as

$$\sigma_r(\epsilon, \xi_1, \xi_2) = \sigma_t(\epsilon) / Z_r(E) \quad (17)$$

with the rotational collision number function  $Z_r(E)$  defined by

$$1/Z_r(E) = \min[1, (4 - \omega) \Delta E_r(E) / E]. \quad (18)$$

The elastic cross section is given by

$$\begin{aligned} \sigma_e(\epsilon, \xi_1, \xi_2) &= \sigma_t(\epsilon) - \sigma_r(\epsilon, \xi_1, \xi_2) \\ &= \sigma_t(\epsilon) [1 - 1/Z_r(E)]. \end{aligned} \quad (19)$$

#### B. Null-collision DSMC procedure

The null-collision DSMC procedure for the MSICS model is described for the molecular collision simulation during a time step  $\Delta t$  in a cell with a volume  $V$  and a molecular number  $N$ .

(a) For the total scattering cross section given by Eq. (4), the maximum value of  $g\sigma_t(\epsilon)$  for all of the collision pair with relative velocity  $\mathbf{g}$  ( $g = |\mathbf{g}|$ ) and translational energy  $\epsilon = \mu g^2/2$ ,  $\mu$  being the reduced mass, is evaluated as

$$\begin{aligned} S_{\max} &= \max[g\sigma_t(\epsilon)], \quad g \leq g_{\max} \\ &= g_{\max} \sigma_t(\epsilon_{\max}), \end{aligned} \quad (20)$$

where  $g_{\max}$  is the maximum value of  $g$  for all the collision pairs and evaluated to be  $2v_{\max}$  from the maximum veloc-

ity  $v_{\max}$  of all the molecules in the cell and  $\epsilon_{\max} = \mu g_{\max}^2/2$ . Assuming that all the collision pairs have the same maximum value of  $S_{\max}$ , the collision frequency (including null collisions)  $\nu$  is given by

$$\nu = (S_{\max}/V)(N^2/2). \quad (21)$$

(b) A time interval  $\Delta t_c$  between successive collisions is given by

$$\Delta t_c = -\ln(R)/\nu, \quad (22)$$

where  $R$  is a uniform random number in the range (0, 1). When the summation of  $\Delta t_c$  exceeds  $\Delta t$ , the molecular collision simulation in the cell ends.

(c) A collision pair is randomly chosen from all the molecules in the cell, because all the collision pairs have the same collision probability per unit time,  $S_{\max}/V$ . If the same molecule is selected, then the collision is taken to be null and the procedure (b) is repeated. The collision is determined to be real or null by the respective probabilities

$$\begin{aligned} P_{\text{real}} &= g\sigma_t(\epsilon)/S_{\max}, \\ P_{\text{null}} &= 1 - P_{\text{real}}. \end{aligned} \quad (23)$$

If the collision is null, then the procedure (b) is repeated. If the collision is real, then the collision is determined to be rotationally inelastic or elastic by the respective probabilities

$$\begin{aligned} P_r &= \sigma_r(\epsilon, \xi_1, \xi_2)/\sigma_t(\epsilon) = 1/Z_r(E), \\ P_e &= \sigma_e(\epsilon, \xi_1, \xi_2)/\sigma_t(\epsilon) = 1 - 1/Z_r(E). \end{aligned} \quad (24)$$

(d) For the rotationally inelastic collision, the rotational energies  $\xi_1'$  and  $\xi_2'$  after collision are assigned by the acceptance-rejection method with the normalized probability function

$$\begin{aligned} P(\xi_1', \xi_2') &= \zeta_r(E, \xi_1', \xi_2')/\max[\zeta_r(E, \xi_1', \xi_2')] \\ &= [1 - (\xi_1' + \xi_2')/E]^{1-\alpha}, \end{aligned} \quad (25)$$

i.e., if  $\xi_1' = R_1 E$  and  $\xi_2' = R_2 E$  satisfy the conditions  $\xi_1' + \xi_2' < E$  and  $R_3 \leq P(\xi_1', \xi_2')$ , then  $\xi_1'$  and  $\xi_2'$  are accepted as the rotational energies after collision, where  $R_1$ ,  $R_2$ , and  $R_3$  are uniform random numbers.

Assigning a deflection angle  $\chi$  from Eq. (5) as

$$\cos\chi = 2R^{1/\alpha} - 1, \quad (26)$$

the velocities after collision  $\mathbf{v}_1'$  and  $\mathbf{v}_2'$  are calculated from the velocities before collision  $\mathbf{v}_1$  and  $\mathbf{v}_2$  of the collision molecules 1 and 2, respectively, as

$$\begin{aligned} \mathbf{v}_1' &= (\mathbf{v}_1 + \mathbf{v}_2)/2 + \mathbf{g}'/2, \\ \mathbf{v}_2' &= (\mathbf{v}_1 + \mathbf{v}_2)/2 - \mathbf{g}'/2, \\ \mathbf{g}' &= (1 - \Delta\xi/\epsilon)^{1/2}(\mathbf{g}\cos\chi + \mathbf{G}\sin\chi), \end{aligned} \quad (27)$$

where  $\Delta\xi = \xi_1' + \xi_2' - \xi_1 - \xi_2$  and  $\mathbf{G} = (G_x, G_y, G_z)$  is given by

$$\begin{aligned} G_x &= -g_{yz}\sin\phi, \\ G_y &= (g_x g_y \sin\phi - g g_z \cos\phi)/g_{yz}, \\ G_z &= (g_x g_z \sin\phi + g g_y \cos\phi)/g_{yz}, \end{aligned} \quad (28)$$

in Cartesian coordinates (x, y, z), in which  $\mathbf{g} = \mathbf{v}_1 - \mathbf{v}_2 = (g_x, g_y, g_z)$ ,  $g_{yz} = (g_y^2 + g_z^2)^{1/2}$ , and  $\phi$  is the azimuthal angle assigned to be  $\phi = 2\pi R$ .

(e) For the elastic collision, the rotational energies are not changed and the velocities after collision are given by Eq. (27) with  $\Delta\xi = 0$ .

(f) If  $v_{\max} \geq \max(|\mathbf{v}_1'|, |\mathbf{v}_2'|)$ , then the procedure (b) is repeated; otherwise the procedure (a) is repeated with  $v_{\max} = \max(|\mathbf{v}_1'|, |\mathbf{v}_2'|)$ .

### C. Rotational relaxation of nitrogen in isothermal bath

The calibration of the MSICS model is made for nitrogen by adjusting the parameter  $Z_r^\infty$  of Parker's rotational energy gain function so that the DSMC calculation of the rotational temperature relaxation in an isothermal bath reproduces reasonably the CTC-DSMC data. The VSS parameters are taken as the low-temperature values for  $T \leq 300\text{K}$  and the high-temperature values for  $T > 300\text{K}$ .

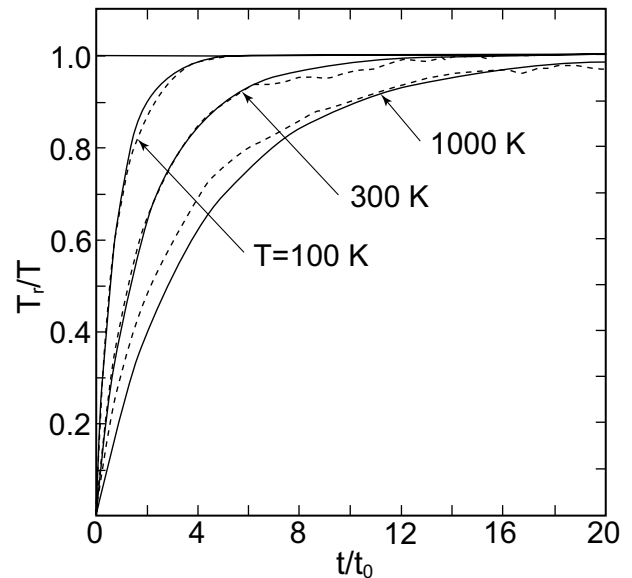


FIG. 5. Rotational temperature relaxation in an isothermal bath obtained by DSMC calculation with the MSICS model (—,  $Z_r^\infty = 10$ ) for the zero initial rotational temperature at the bath temperature  $T = 100, 300$ , and  $1000\text{K}$  as compared with the CTC-DSMC data for the PES8 potential (---).

Because the MSICS model may be too simple to reproduce the details of the CTC-DSMC data over a wide range of bath temperatures, the calibration is made in an appropriate range of bath temperatures. In the present paper, the calibration is made mainly at  $T=300\text{K}$  and the value of  $Z_r^\infty$  is determined to be 10. Figure 5 shows that the rotational temperature relaxation for  $Z_r^\infty=10$  compares fairly well with the CTC-DSMC data for  $T=100$ , 300, and 1000K, where the DSMC molecular number  $N$  is taken to be a large value of  $10^6$  by taking account of the computational efficiency of the MSICS model.

A comparison of the relative rotational distribution function  $(y_j/g_j)/(y_0/g_0)$  with the CTC-DSMC data is presented in Fig. 6 for  $T=300\text{K}$ . It is indicated that the agreement is reasonable at the early ( $t/t_0 < 0.5$ ) and final ( $t/t_0 > 4$ ) relaxation stages but at the middle stage ( $0.5 < t/t_0 < 4$ ) the MSICS distribution function follows somewhat inadequately the CTC-DSMC relaxation to the Boltzmann distribution function. The DSMC rotational distribution

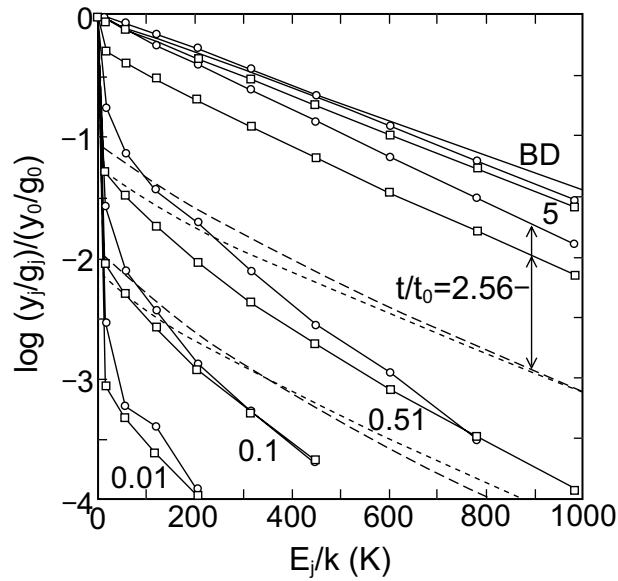


FIG. 6. Relaxation of rotational distribution function in an isothermal bath obtained by DSMC calculation with the MSICS model ( $\square$ ,  $Z_r^\infty=10$ ) for the zero initial rotational temperature at the bath temperature  $T=300\text{K}$  as compared with the CTC-DSMC data for the PES8 potential ( $\circ$ ). The rotational distribution functions obtained by DSMC calculations with the  $Z_r=5.6$  (---) and  $p(\epsilon_c)$  (- - -) probability models (Ref. 6) for the initial rotational temperature of 2.9K at  $T=300\text{K}$  are plotted at the time  $t=\tau_e$  ( $t/t_0=0.51$ ) and  $t=5\tau_e$  ( $t/t_0=2.56$ ). BD denotes the Boltzmann distribution function at the bath temperature.

functions obtained by Wysong and Wadsworth<sup>6</sup> using the constant ( $Z_r=5.6$ ) and variable  $[p(\epsilon_c)]$  probability models of Borgnakke-Larsen type for the initial rotational temperature of 2.9K at  $T=300\text{K}$  are plotted at the time  $t=\tau_e$  ( $t/t_0=0.51$ ) and  $t=5\tau_e$  ( $t/t_0=2.56$ ). It is observed that the rotational relaxation is slower for the  $Z_r=5.6$  and  $p(\epsilon_c)$  models than for the MSICS model.

#### D. Rotational relaxation of nitrogen through normal shock wave

The MSICS model is applied to the DSMC calculation of the rotational relaxation of nitrogen through a Mach 12.9 shock wave to compare the MSICS results with the CTC-DSMC data and experimental measurements.<sup>8</sup> The VSS parameters are taken as the low-temperature values. The cell width  $\Delta x$  is taken to be the same as that employed in the CTC-DSMC calculation but the average molecular number per cell is taken to be a large value of about 1000.

The profiles of normalized number density  $\bar{n}$ , translational temperature  $\bar{T}$ , and rotational temperature  $\bar{T}_r$  are shown in Fig. 7 as compared with the CTC-DSMC data and the measured data of  $\bar{n}$  and  $\bar{T}_r$ . A comparison between

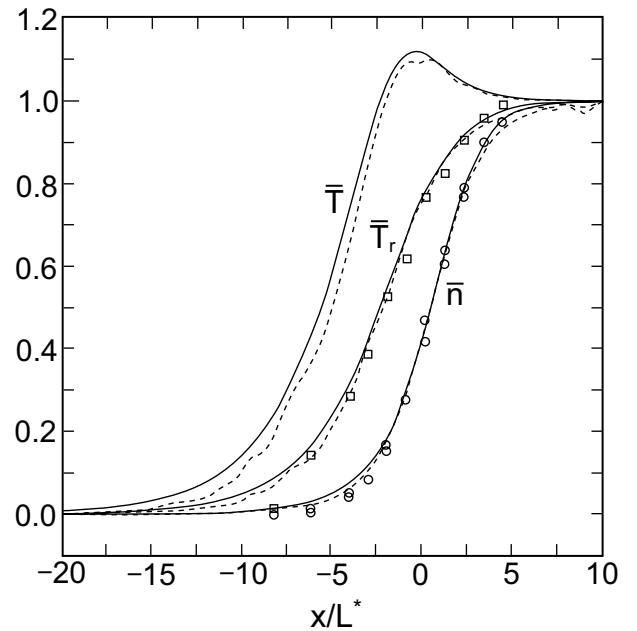


FIG. 7. Profiles of normalized number density ( $\bar{n}$ ) and translational ( $\bar{T}$ ) and rotational ( $\bar{T}_r$ ) temperatures through a Mach 12.9 shock wave obtained by DSMC calculation with the MSICS model ( $-$ ,  $Z_r^\infty=10$ ) as compared with the CTC-DSMC data for the PES8 potential ( $- - -$ ) and the experimental data (Ref. 8) of  $\bar{n}$  ( $\circ$ ) and  $\bar{T}_r$  ( $\square$ ).

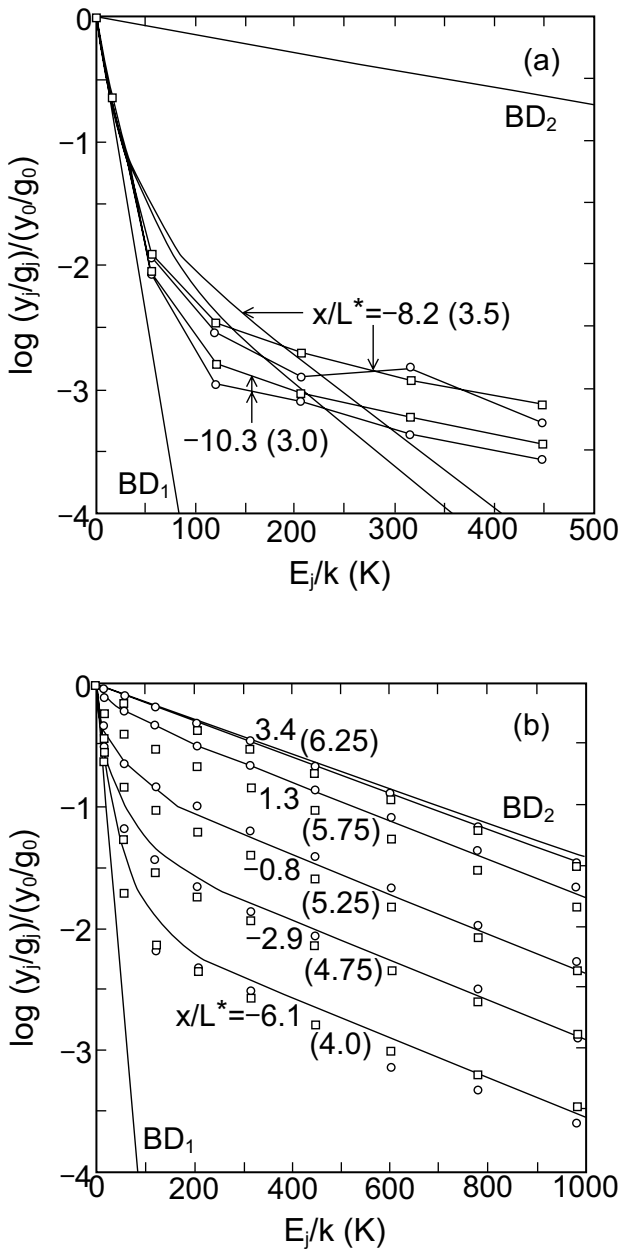


FIG. 8. Relaxation of rotational distribution function through a Mach 12.9 shock wave obtained by DSMC calculation with the MSICS model ( $\square$ ,  $Z_r^\infty=10$ ) as compared with the CTC-DSMC data for the PES8 potential ( $\circ$ ) and the experimental data ( $-$ , Ref. 8). The value in parentheses is the measured position in the unit of turns.  $BD_1$  and  $BD_2$  denote the Boltzmann distribution functions at the upstream and downstream temperatures, respectively.

the MSICS profiles and the CTC-DSMC data indicates that the MSICS profiles rise a little faster than the CTC-DSMC data in the front portion of the shock wave. It is pointed out that the agreement with the experimental measurements is considerably better for the MSICS model than for the SICS model (Fig. 4 of Ref. 14) and the  $Z_r=5.6$  and  $p(\epsilon_c)$  models (Fig. 8 of Ref. 6).

The relaxation of the relative rotational distribution function  $(y_i/g_i)/(y_0/g_0)$  is presented in Fig. 8 as compared with the CTC-DSMC data and experimental measurements. In the upstream portion of the shock wave,  $x/L^* = -10.3$  (3.0 turns) and  $-8.2$  (3.5 turns), the MSICS distribution function agrees fairly well with the CTC-DSMC data and reveals a large deviation from the experimental data at the high quantum numbers. In the middle portion of the shock wave, the MSICS distribution function shows a bimodal form consistent with the CTC-DSMC and measured data but relaxes to the Boltzmann distribution function somewhat slower than the CTC-DSMC and measured data.

#### IV. CONCLUDING REMARKS

The CTC-DSMC method is applied to the simulation of the rotational relaxation of nitrogen in an isothermal bath and through a normal shock wave using an improved intermolecular potential. The bath calculation makes a set of rotational relaxation data over a wide range of bath temperatures. The shock wave calculation reproduces well the experimental measurements except in the upstream portion of the shock wave. The CTC-DSMC data may serve as a physically accurate database for the assessment and improvement of DSMC rotational relaxation models.

The MSICS model is derived by modifying the SICS model for the continuous rotational energy and the value of the adjustable parameter of Parker's energy gain function is determined for nitrogen by fitting the rotational temperature relaxation in an isothermal bath to the CTC-DSMC data over an appropriate range of bath temperatures. The MSICS model is applied to the DSMC calculation of the rotational relaxation of nitrogen through a normal shock wave to see the agreement with the CTC-DSMC data and experimental measurements. Because the MSICS model shows an improvement over the SICS model in the agreement with the experimental shock wave measurements, it may be of interest to apply the

MSICS model to DSMC calculations of the rotational relaxation in rarefied gas flows. It should be remarked that some simple expressions for the rotational collision number function  $Z_r(E)$  are assessed using the CTC-DSMC database but no other expression is found to be preferable to that derived from Parker's energy gain function.

## ACKNOWLEDGMENTS

The author would like to thank Dr. Ingrid J. Wysong for useful information on intermolecular potentials and informative discussions and Mr. Shinichi Kojima for making an efficient program to evaluate the PES8(AWJ) potential.

## REFERENCES

- 1) G.A. Bird, *Molecular Gas Dynamics and the Direct Simulation of Gas Flows* (Clarendon, Oxford, 1994).
- 2) C. Borgnakke and P.S. Larsen, "Statistical collision model for Monte Carlo simulation of polyatomic gas mixture," *J. Comput. Phys.* **18**, 405 (1975).
- 3) K. Koura, "Statistical inelastic cross-section model for the Monte Carlo simulation of molecules with discrete internal energy," *Phys. Fluids A* **4**, 1782 (1992).
- 4) I.D. Boyd, "Relaxation of discrete rotational energy distributions using a Monte Carlo method," *Phys. Fluids A* **5**, 2278 (1993).
- 5) T. Tokumasu and Y. Matsumoto, "Dynamic molecular collision (DMC) model for rarefied gas flow simulations by the DSMC method," *Phys. Fluids* **11**, 1907 (1999).
- 6) I.J. Wysong and D.C. Wadsworth, "Assessment of direct simulation Monte Carlo phenomenological rotational relaxation models," *Phys. Fluids* **10**, 2983 (1998).
- 7) M.L. Strekalov, "Rotational relaxation and collisional energy transfer calculations based on a new fitting law," *Mol. Phys.* **86**, 39 (1995).
- 8) F. Robben and L. Talbot, "Experimental study of the rotational distribution function of nitrogen in a shock wave," *Phys. Fluids* **9**, 653 (1966).
- 9) K. Koura, "Monte Carlo direct simulation of rotational relaxation of diatomic molecules using classical trajectory calculations: Nitrogen shock wave," *Phys. Fluids* **9**, 3543 (1997).
- 10) K. Koura, "Monte Carlo direct simulation of rotational relaxation of nitrogen through high total temperature shock waves using classical trajectory calculations," *Phys. Fluids* **10**, 2689 (1998).
- 11) K. Koura, "Direct simulation Monte Carlo method coupled with classical trajectory calculations for rigid diatomic molecules: Application to nitrogen shock wave," *Rarefied Gas Dynamics* **21**, edited by R. Brun, R. Campargue, R. Gatignol, and J.C. Lengrand (CÉPADUÈS-ÉDITIONS, Toulouse, 1999), Vol. II, p.23.
- 12) A. van der Avoird, P.E.S. Wormer, and A.P.J. Jansen, "An improved intermolecular potential for nitrogen," *J. Chem. Phys.* **84**, 1629 (1986).
- 13) D. Cappelletti, F. Vecchiocattivi, F. Pirani, E.L. Heck, and A.S. Dickinson, "An intermolecular potential for nitrogen from a multi-property analysis," *Mol. Phys.* **93**, 485 (1998).
- 14) K. Koura, "Statistical inelastic cross-section model for the Monte Carlo simulation of molecules with continuous internal energy," *Phys. Fluids A* **5**, 778 (1993).
- 15) K. Koura, "Rotationally and vibrationally inelastic cross-section models for the direct simulation Monte Carlo method," *Rarefied Gas Dynamics* **20**, edited by C. Shen (Peking UP, Beijing, 1997), p. 719.
- 16) K. Koura and H. Matsumoto, "Variable soft sphere molecular model for inverse-power-law or Lennard-Jones potential," *Phys. Fluids A* **3**, 2459 (1991).
- 17) K. Koura and H. Matsumoto, "Variable soft sphere molecular model for air species," *Phys. Fluids A* **4**, 1083 (1992).
- 18) K. Koura, "Null-collision technique in the direct-simulation Monte Carlo method," *Phys. Fluids* **29**, 3509 (1986).
- 19) K. Koura, "A sensitive test for accuracy in evaluation of molecular collision number in the direct-simulation Monte Carlo method," *Phys. Fluids A* **2**, 1287 (1990).
- 20) K. Koura, "Direct simulation Monte Carlo study of quantum effects on the spherical expansion of  $^4\text{He}$ ," *Phys. Fluids* **11**, 3174 (1999).
- 21) M.D. Pattengill, "A comparison of classical trajectory and exact quantal cross sections for rotationally inelastic Ar- $\text{N}_2$  Collisions," *Chem. Phys. Lett.* **36**, 25 (1975).

- 22) I.J. Wysong, private communication.
- 23) I.J. Wysong and D.C. Wadsworth, "Assessment of rotational collision number of nitrogen at high temperatures and its possible effect on modeling of reacting shocks," *Rarefied Gas Dynamics* **21**, edited by R. Brun, R. Campargue, R. Gatignol, and J.C. Lengrand (CÉPADUÈS-ÉDITIONS, Toulouse, 1999), Vol. II, p.321.
- 24) J.G. Parker, "Rotational and vibrational relaxation in diatomic gases," *Phys. Fluids* **2**, 449 (1959).
- 25) K. Koura, "A generalization for Parker rotational relaxation model based on variable soft sphere collision model," *Phys. Fluids* **8**, 1336 (1996).

## APPENDIX

In order to make a further database for the assessment and improvement of DSMC rotational relaxation models, the Monte Carlo simulation of the translational and rotational relaxation of nitrogen test-particles (TP) in an isothermal (equilibrium) heat-bath of nitrogen is performed using classical trajectory calculations and the PES8 potential. The test-particles initially have the Maxwell (translational) and Boltzmann (rotational) distribution functions at the initial temperature  $T_0$  and are infinitely dilute in bath molecules maintaining the constant bath temperature  $T_b$ .

Because the interaction between test-particles may be ignored, the test-particle Monte Carlo (TPMC) method [K. Koura, *Phys. Fluids* **6**, 3473 (1994)] is employed instead of the DSMC method and coupled with classical trajectory calculations (CTC). The CTC-TPMC calculations are made on the parallel computing system with the total number of test-particles  $N=33600$ .

The relaxation of the translational and rotational temperatures in the heating ( $T_0 < T_b$ ) and cooling ( $T_0 > T_b$ ) processes is shown in Figs. A1–A5 for the initial and bath temperatures (50K, 100K), (50K, 300K), (100K, 300K), (300K, 500K), and (300K, 1000K), where the time  $t$  is normalized by the collision time  $t_b = [n_b \pi \sigma_{LJ}^2 (2kT_b/m)^{1/2}]^{-1}$ ,  $n_b$  being the bath number density. As is expected, the rotational temperature approaches the bath temperature slower than the translational temperature and the rotational relaxation becomes slower with increasing the initial and bath temperatures. It is of interest to note that the rotational relaxation is slower in the heating process than in the cooling process at low temperatures ( $\leq 500K$ ) but, at high temperatures ( $\geq 1000K$ ), the rotational relaxation is slower in the cooling process than in the heating process. It should be remarked that available DSMC rotational relaxation models may not simultaneously reproduce the heating and cooling results.

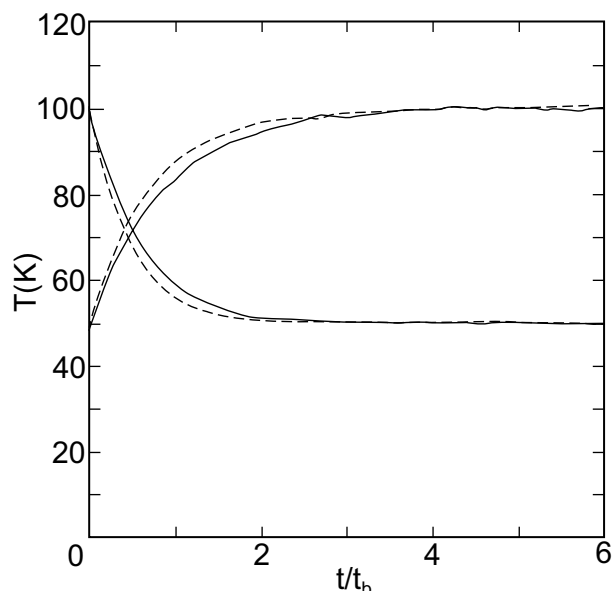


FIG. A1. Relaxation of translational (---) and rotational (—) temperatures in the heating and cooling processes for the initial and bath temperatures (50K, 100K).

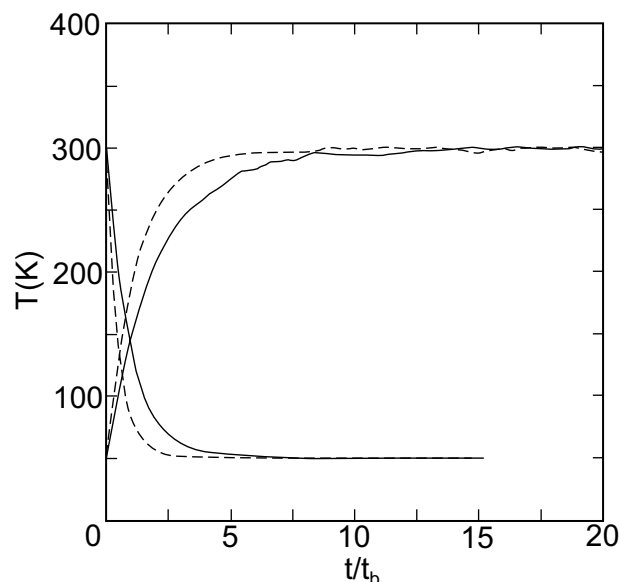


FIG. A2. Same as Fig. A1; (50K, 300K).

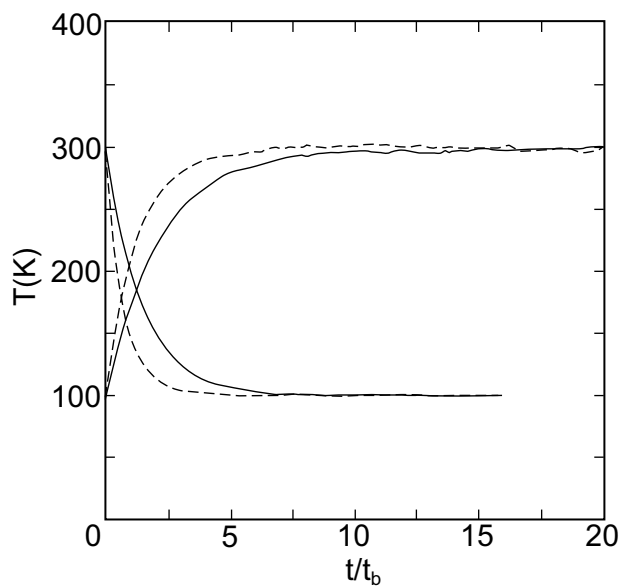


FIG. A3. Same as Fig. A1; (100K, 300K).

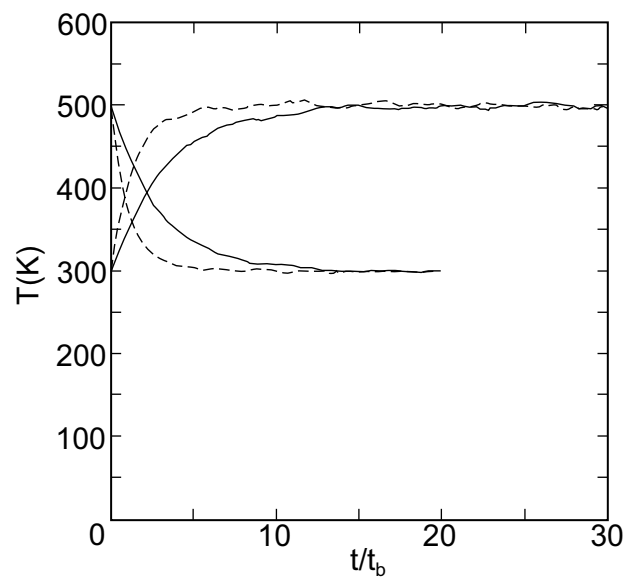


FIG. A4. Same as Fig. A1; (300K, 500K).

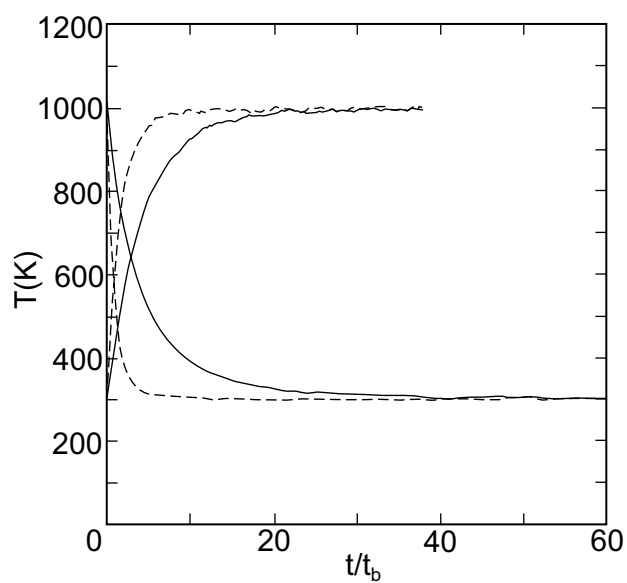


FIG. A5. Same as Fig. A1; (300K, 1000K).





JAXA Research and Development Report JAXA-RR-07-001E

---

Date of Issue : 31 July, 2007

Edited and Published by : Japan Aerospace Exploration Agency

7-44-1 Jindaiji-higashimachi, Chofu-shi, Tokyo 182-8522, Japan

URL : <http://www.jaxa.jp/>

Printed by : Kyoushin Co., Ltd.

---

Inquires about copyright and reproduction should be addressed to the  
Aerospace Information Archive Center, Information Systems Department,  
JAXA.

2-1-1 Sengen, Tsukuba-shi, Ibaraki 305-8505, Japan

phone : +81-29-868-5000 fax : +81-29-868-2956

---

Copyright © 2007 by JAXA.

All rights reserved. No part of this publication may be reproduced, stored in  
retrieval system or transmitted, in any form or by any means, electronic,  
mechanical, photocopying, recording, or otherwise, without permission in  
writing from the publisher.



Printed on Recycled Paper